Hypoxia-inducible C-to-U coding RNA editing downregulates *SDHB* in monocytes

BACKGROUND: RNA editing is a post-transcriptional regulatory mechanism that can alter the coding sequences of certain genes in response to physiological demands. Most RNA editing occurs in the form of A-to-I conversion, whereas C-to-U RNA editing, especially within the coding sequences, is rare in mammals. We previously identified C-to-U RNA editing (C136U, R46X) which inactivates a small fraction of succinate dehydrogenase (SDH; mitochondrial complex II) subunit B gene (*SDHB*) mRNAs in normal steady-state peripheral blood mononuclear cells (PBMCs). SDH is a heterotetrameric tumor suppressor complex which when mutated causes paraganglioma tumors that are characterized by constitutive activation of hypoxia inducible pathways. Here, we studied regulation, extent and cell type origin of *SDHB* RNA editing. METHODS: We used short-term cultured PBMCs obtained from random healthy donors, performed monocyte enrichment by cold aggregation, and employed a novel allele-specific quantitative PCR method, flow cytometry, immunologic cell separation, gene expression microarray, database analysis and high-throughput RNA sequencing. RESULTS: While the editing rate is low in uncultured monocyte-enriched PBMCs (average 2.0%, range 0.4%-6.3%, n=42), it is markedly upregulated upon 2-day exposure to hypoxia (average 18.2%, range 2.8%-49.4%, n=14) and during macrophage differentiation in normoxia peaking on culture days 5 and 6 (average 10.1%, range 2.7%-18.8%, n=17). Further purified CD14-positive monocytes showed increased percentages of C136U transcripts by 1.25-fold in normoxic cultures and 1.68-fold in hypoxic cultures (n=4). CD14-negative lymphocytes showed no evidence of *SDHB* editing. The *SDHB* genomic DNA remained wild-type during increased RNA editing. Microarray analysis showed expression changes in genes of wound healing and immune response pathways as the editing rate increased in normoxic cultures. High-throughput sequencing of *SDHB* and *SDHD* transcripts confirmed the induction of C136U RNA editing but showed no additional verifiable coding edits. Bioinformatic analysis of *SDHB* RNA sequence data from 16 normal human tissues from the Illumina Body Map and from 45 samples representing 23 different cell types from the ENCODE projects confirmed the occurrence of site-specific C136U editing in whole blood (1.7%) and two primary

CD14+ monocyte samples (1.9% and 2.6%). In contrast, the other cell types showed an average of 0.2% and 0.1% C136U editing rates in the two databases, respectively. CONCLUSIONS: These findings demonstrate that C-to-U coding RNA editing of certain genes is dynamically induced by physiologically relevant environmental factors and suggest that epigenetic downregulation of *SDHB* by site-specific RNA editing plays a role in hypoxia adaptation of monocytes.

Bora E. Baysal[1,†], Kitty De Jong[1], Biao Liu[2], Jianmin Wang[2], Santosh K. Patnaik[3], Paul K. Wallace[1], R. Thomas Taggart[1]

Departments of Pathology and Laboratory Medicine[1] Biostatistics and Bioinformatics[2] and Thoracic Surgery[3], Roswell Park Cancer Institute, Buffalo, NY 14263, USA

[†]*To whom correspondence should be addressed:*

Bora E. Baysal, MD, PhD

Department of Pathology, Roswell Park Cancer Institute

Elm & Carlton Streets, Buffalo, NY 14263, USA

Tel: 716-845-3204; Email:bora.baysal@roswellpark.org

INTRODUCTION

RNA editing is a post-transcriptional regulatory mechanism which often results in conversion of adenosine to inosine (A-to-I) (Nishikura 2010). Recent whole transcriptome sequence analyses reveal abundant A-to-I type RNA editing in non-coding and Alu-containing transcript regions while RNA editing of protein encoding regions, especially of non-A-to-I types, appears to be very rare (Kleinman, Adoue & Majewski 2012; Piskol, et al., 2013). Site-specific C-to-U RNA editing leading to amino acid recoding of an endogenous gene in normal mammalian cells was previously confirmed, to our knowledge, only in the *APOB* gene encoding apolipoprotein B (Blanc & Davidson 2003). C-to-U editing of *APOB* is catalyzed by APOBEC1 cytidine deaminase that generates a shorter protein isoform in intestinal epithelial cells. APOBEC1 also inactivates 4%-17% of neurofibromatosis type 1 (*NF1*) gene transcripts by site-specific C-to-U RNA editing in certain high-grade NF1 tumors but not in normal cells (Skuse, et al., 1996).

We previously identified *SDHB* C-to-U mRNA editing (C136U) at low steady-state levels in peripheral blood mononuclear cells (PBMCs) of normal individuals using reverse transcription (RT) and semi-quantitative PCR (Baysal 2007). Analysis of the purified PBMC subsets in a single donor showed that the C136U editing rate was higher in monocytes than in lymphocytes. SDH is a central metabolic enzyme in Krebs cycle (Rutter, Winge & Schiffman 2010) and a tumor suppressor for hereditary paraganglioma (PGL) (Baysal, et al., 2000). SDH catalyzes the oxidation of succinate to fumarate during aerobic respiration. In anaerobically respiring mitochondria of lower organisms, SDH is inactive and fumarate is often reduced to succinate in a reverse reaction catalyzed by fumarate reductase (Muller, et al., 2012). Germline inactivating mutations in the nuclear-encoded SDH subunit genes, primarily in *SDHB* and *SDHD*, cause PGL tumors (Burnichon, et al., 2012) which show constitutive activation of the hypoxia-inducible pathways. PGL tumors recapitulate the

high-altitude associated carotid body (CB) paragangliomas (Saldana, Salem & Travezan 1973), increase in severity with increased altitudes (Astrom, et al., 2003; Cerecer-Gil, et al., 2010) and share transcriptome characteristics with Von-Hippel Lindau (VHL) disease tumors (Dahia, et al., 2005). The VHL gene product plays an important role in normoxic degradation of hypoxia-inducible factors (HIFs) (Kaelin & Ratcliffe 2008). Succinate and reactive oxygen species that accumulate upon SDH inactivation were implicated as downstream messengers leading to stabilization of HIF1α in normoxic conditions (Selak, et al., 2005; Guzy, et al., 2008) although mechanisms of PGL tumorigenesis remains unconfirmed.

The *SDHB* C136U RNA editing converts a highly conserved arginine residue to a premature stop codon (R46X) shortly after the mitochondrial targeting signal and inactivates the *SDHB* gene product, the iron-sulfur subunit of the SDH complex. The R46X germ line mutation was previously described in multiple index patients with PGL confirming its pathogenicity (Bayley, Devilee & Taschner 2005). Here, we studied the *SDHB* C136U transcript editing in short-term cultured PBMCs using a novel allele specific quantitative PCR assay (AS qPCR), high-throughput genetic methods, immunophenotyping, immunoseparation, morphology and database analysis. Our aim was to determine the prevalence, distribution, cell type origin and other factors influencing *SDHB* editing using a reproducible assay to gain functional insights. We found that *SDHB* C136U editing is present at low levels in fresh uncultured total and monocyte-enriched PBMCs, but it markedly increases during macrophage differentiation *in vitro* and upon short-term hypoxic exposure in monocytes. These results provide unprecedented evidence that functional transcript dosage for a central metabolic enzyme is regulated by environmentally-inducible site-specific C-to-U RNA editing.

MATERIALS AND METHODS

PBMC isolation and cell culture

Leukocytes were isolated from Trima leukoreduction filters (Terumo BCT, Lakewood, CO) of anonymous healthy platelet donors following an IRB review and determination as non-human subject research. PBMCs were purified by histopaque 1077 (Sigma-Aldrich, St. Louis, MO) and washed twice with RPMI-1640/10% fetal bovine serum (FBS) to remove residual platelets. Each filter often gave $5X10^8$ or more PBMCs. Monocytes were enriched by the cold aggregation method (Mentzer, et al., 1986) with certain modifications. PBMCs were suspended in 35 ml RPMI-1640 in a 50 ml polypropylene tube and incubated at 4 ºC for 1 h on a rocker panel for homotypic aggregation of monocytes. For monocyte enrichment, the tube was positioned upright, underlaid with 6 ml FBS and incubated overnight at 4 ºC. The cell precipitate under the serum was collected for culture. Monocyte enrichment was approximately 70% (n=5) by short-term precipitation (up to 3 hours) and 27% (n=10) by overnight precipitation over serum as determined by percentages of the CD14+ cells by flow cytometry. The non-aggregating upper layer was markedly depleted of monocytes (less than 4%, n=3). We used the overnight precipitation method which gave higher yield of total cells and were associated with higher levels of C136U editing in culture. Precipitated cells under the serum were centrifuged for 10 min at 250xg and suspended in 20 ml RPMI-1640 with 10% FBS and penicillin/streptomycin. Cell density was calculated by a hemocytometer (improved Neubauer , InCyto, Covington, GA). After further dilution, two milliliters of the cell suspension was distributed to each well of a six-well tissue culture plate (Costar, Corning Incorporated, Corning, NY). Editing rates were determined in daily collected individual wells. We cultured 21-30x10^6 cells/2 ml per well (also see results). Cultures were incubated at, 5% CO_2 with either 21% O_2 (normoxia) or 1% O_2 combined with 94% nitrogen (hypoxia). Hypoxic cultures were pre-incubated at 37 ºC, 21% O_2 for

approximately 3 hours before being placed in the hypoxia chamber (XVIVO system, BioSpherix, Lacona, NY). Fresh culture media was added after 7 days in culture.

The THP-1 monocytic leukemia cell line was purchased from ATCC (Manassas, VA). Various cytokines/differentiating agents were added for the following final concentrations: macrophage colony stimulating factor (M-CSF; 50 ng/ml), granulocyte-macrophage (GM)-CSF (50 ng/ml), interleukin 4 (IL4; 50 ng/ml, vitamin D (10 nM), retinoic acid (1 µM), PMA (4-beta-phorbol-12-myristate-13-acetate; 100 nM). Cytokines were purchased from Peprotech (Rocky Hill, NJ) and differentiating agents were purchased from Sigma-Aldrich.

Microscopy and imaging

Standard tissue culture monitoring and imaging was performed using an Axio microscope (Zeiss, Jena, Germany). Adherent aggregates (approximately 100 micron or larger in diameter) were counted at low power (2.5X) magnification. Live image photographs were taken using a Leica AF6000LX system (Houston, TX) which is comprised of a Leica DMI-6000B microscope and Leica LAS AF software interface.

Nucleic acid isolation and analysis

RNA and DNA were isolated using Trizol (Life Technologies, Grand Island, NY) and DNA Wizard genomic DNA purification kit (Promega, Madison, WI), respectively. Nucleic acid lysis buffer or Trizol was added directly to the adherent cells in plate well. Nucleic acid was quantified by a spectrophotometer (Nanondrop, Thermo Scientific, Wilmington, DE). Oligonucleotide primers and templates were obtained from IDT Technologies (Coralville, IA).

RT and qPCR were performed following the manufacturer's kits and instructions (LightCycler 480II, Roche, Indianapolis, IN). Complementary DNA from total RNA (1-2 µg) was synthesized using a mixture of random hexanucleotide and oligo-dT_{12} primer mixture. qPCR amplification of cDNAs was performed and crossing point (Cp) levels of C136U (T assay) and total *SDHB* (total assay) were determined separately. Each assay was performed in duplicate or triplicate wells. T assay and total assay had the same forward oligonucleotide primer for *SDHB* exon 1 and different oligonucleotide reverse primers in exon 2, where the C136U editing occurs. The reverse primer for the T assay had an extra T at its 3'-end relative to the reverse primer in the common assay. (Oligonucleotide primers and probes used in this study are listed in supplemental Table S1.)

The relative amount of the edited transcripts was calculated by the delta-Cp method by exponentiating the total transcript Cp minus the edited transcript Cp value to the power of 2. This approach assumes 100% duplication efficiency per cycle in both assays. Control PCR reactions were performed to test the specificity and amplification efficiency of oligonucleotide primer pairs using synthetic oligonucleotide templates. Assays with 8-fold serially diluted synthetic oligonucleotide templates for the wild-type and C136T edited sequences showed a duplication efficiency of 107% for both total and T assays between 1 femtomole and 0.245 attomole (Supplemental Table S2). The mutation-specific primer had a high specificity for the edited transcripts, with an average false positive amplification rate of 1.38% when the control wild type oligonucleotide template sequence was amplified in an over 25,000-fold concentration range. When 100% T template was used, the average estimate of the C136U edited transcripts was 91% between 8 femtomoles and 0.245 attomoles. These control experiments suggest that AS qPCR estimates may be slightly lower than the true editing rates. We chose this stringent AS qPCR method to ensure we did not overestimate the C136U editing rates. The estimated percentage of edited transcripts using this method was highly

reproducible in biological samples. For example, a set of 14 samples containing both low and high levels of edited transcripts gave very similar results in two replicate experiments with a Pearson correlation coefficient of 99.4%. In each assay, a positive control sample which had a mutation rate of 15%-17% was included. Relative quantification of cytidine deaminase (*CDA)* and *SDHB* mRNA expression was performed by 2^(-delta delta(Ct)) method (Livak & Schmittgen 2001) using expression levels of the housekeeping *B2M* beta-2 microglobulin transcripts for normalization.

Microarray analysis of gene expression

Expression profiling was accomplished using the Human HT-12 whole-genome gene expression array and direct hybridization assay (Illumina, San Diego, CA). Initially, 500 ng total RNA was converted to cDNA, followed by in vitro transcription to generate biotin-labeled cRNA using the Ambion Illumina TotalPrep RNA Amplification Kit (Ambion, Austin, TX) as per manufacturer's instructions. 750 ng of the labeled probes were then mixed with hybridization reagents and hybridized overnight at 58 °C to the HT-12v4 BeadChips. Following washing and staining with Cy3-streptavidin conjugate, the BeadChips were imaged using the Illumina iScan Reader to measure fluorescence intensity at each probe. The intensity of the signal corresponds to the quantity of the respective mRNA in the original sample.

The background corrected gene expression levels were extracted from BeadChip using Illumina's Genome Studio (v2011.1) gene expression module (v1.9.0). The $\log_2$-transformed expression levels were quantile normalized using lumi Bioconductor package in R (Du,Kibbe & Lin 2008) For data quality control, we excluded the genes with detection P value greater than 0.05 (i.e., indistinguishable from the background noise). 18941 out of 34686 genes passed this filtering for downstream analysis.

The limma Bioconductor package (Smyth 2004) was used to calculate the level of differential gene expression. Briefly, a linear model was fit to the data (paired design, with cell means corresponding to the different condition and a random effect for array) and selected contrasts of condition (i.e., case vs. control) were performed. A list of differentially expressed genes with $P < 0.05$ and ≥ 2 fold-change was obtained and analyzed for enriched Gene Ontology (GO) categories and KEGG pathways using NCBI DAVID Bioinformatics Resources (Huang da,Sherman & Lempicki 2009) . The enriched GO terms and KEGG pathways with $P < 0.05$ and ≥ 5 genes were kept.

Accession number

Microarray data have been deposited in the NCBI Gene Expression Omnibus (www.ncbi.nlm.nih.gov/geo/) under accession number GSE45900.

High-throughput RT-PCR amplicon sequencing

SDHB and *SDHD* gene transcripts were amplified by RT-PCR with oligonucleotide primers targeting 5'- and 3'-untranslated regions (primer sequences can be obtained from authors) using Transcriptor reverse transcriptase (Roche) and Ultra2 *Pfu* high fidelity DNA polymerase (Agilent, Santa Clara, CA) . Libraries were preparedusing the Nextera XT DNA sample preparation kit (Illumina) for hHigh-throughput sequencing was on a MiSeq personal sequencing platform (Illumina).

Flow cytometry

Cells ($0.5\text{-}1 \times 10^6$) were pelleted by centrifugation at 400g for 5 minutes and incubated for 20 minutes at room temperature in a total volume of 100 µl with a titrated cocktail of allophycocyanin (APC)-conjugated mouse anti-CD14 antibody (Invitrogen, Carlsbad, CA), Brilliant-violet 421 conjugated CD16 (BioLegend, San Diego, CA), phycoerythrin (PE)-conjugated mouse anti-CD163 antibody (Trillium Diagnostics, Brewer, ME), fluorescein isothiocyanate (FITC)-conjugated mouse

anti-CD206 (BD Biosciences, San Jose, CA), and PE-Cy7-conjugated mouse anti-HLA-DR antibody (BD Biosciences), followed by a wash in phosphate buffered saline (PBS; pH 7.4) and resuspension in 500 µl PBS. Viability is assessed by Live/Dead Yellow (Invitrogen). Flow cytometric acquisition was performed on a FACS Aria I flow cytometer (BD Biosciences) equipped with four laser excitation sources (405 nm at 30 mW; 488 nm at 15 mW; 561 nm at 30 mW, and 631 nm at 17 mW) that was quality-controlled on a daily basis by using BD cytometer setup and tracking beads and FACS DiVa software (BD Biosciences). The filter configurations for the PMTs measuring fluorescence emission of the applied fluorochromes were 450/50 nm (Brilliant-violet 421); 530/30 nm (FITC); 582/15 nm (PE); 780/60 nm (PE-Cy7); and 660/20 nm (APC). Autofluorescence and single-color controls were acquired to perform spectral overlap compensation using the automated compensation matrix feature in FACS DiVa software. A forward scatter threshold was applied to eliminate electronic noise and small particles from the flow cytometric acquisition. A total of 20,000 scatter-inclusive events were acquired for each specimen. Data analysis was performed with FlowJo software version 10.0.4 (Tree Star, Ashland, OR).

Isolation of CD14+ monocytes

Monocytes were isolated either by flow cytometric gating of CD14+ cells (both dim and strong intensity) on a BD FACS Aria I flow sorter, or by CD14 microbeads (Miltenyi Biotec Inc. Auburn, CA) following manufacturer's protocol. Flow cytometry showed 93% or higher purity after CD14 purification.

Immunocytochemical staining

PBMCs were grown in tissue culture chamber slides (Labtek, Scotts Valley, CA). Before staining, medium was aspirated and adherent cells were washed once with PBS. Adherent cells were fixed by

alcohol-based cytology fixative (Leica) and air dried. For antigen retrieval, slides were heated in the steamer for 20 minutes in a citrate buffer (pH 6.0), followed by a 20 minute cool down. Endogenous peroxidase was quenched with aqueous 3% H_2O_2 for 10 minutes and washed with PBS with 0.05% Tween 20 (Sigma). Slides were loaded on anautostainer (Dako, Carpinteria, CA) and a serum-free protein blocker (catalog #X0909, Dako) was applied for 5 minutes, blown off, and the antibody applied for one-hour. Biotinylated goat anti-mouse IgG (Jackson Immuno Research Labs, catalog #115-065-062) was applied for 30 minutes, followed by the Vectastatin Elite ABC Kit (Vector Labs, Burlingame, CA) for 30 minutes, and the 3, 3'-diaminobenzidene chromagen (Dako) for 5 minutes. Finally, the slides were counterstained with hematoxylin, dehydrated, cleared and cover slipped.

Western blot analysis

Cell lysates were prepared using 75 µl of M-PER protein extraction reagent (Thermo, Waltham, MA) per approximately $20X10^6$ washed cells. The concentration of proteins in lysates was determined with the colorimetric Pierce 660 nm protein assay (Thermo). For electrophoresis, lysates (40–60 µg of protein) were boiled for 5 min in buffer containing 50 mM Tris, 2% SDS and 143 mm β-mercaptoethanol. After electrophoresis in Mini-PROTEAN™ TGX pre-cast 4%–15% gradient polyacrylamide gels (Bio-Rad, Hercules, CA) at 15–30 mA for 90 min, proteins were transferred overnight at 30 mA in 10% methanol-containing Tris-glycine buffer to 0.45 µ polyvinylidene difluoride membrane (GE Healthcare, Little Chalfont, UK). For immunoblotting, membranes were blocked in Tris-buffered saline (TBS; 10 mM Tris-HCl and 150 mM NaCl at pH 7.4) with 0.05% Tween-20 and 5% non-fat milk (Carnation™, Nestle, Vevey, Switzerland), and then incubated in the same solution with a primary mouse monoclonal anti-SDHB antibody (ab14714, Abcam, Cambridge, MA) at room temperature for an hour. After washing in TBS/Tween-20 for 30 minutes, membranes were incubated in TBS/Tween-20/milk with a horseradish peroxidase-conjugated

secondary antibody for 1 hour at room temperature. Membranes were then washed in TBS/Tween-20 for 30 min, incubated in Luminata Forte™ chemiluminescence reagent (Thermo), and exposed to photographic film (Thermo). Mouse anti-beta-actin (clone C4, Santa Cruz Biotechnology, Dallas, TX) and horseradish peroxidase-conjugated goat anti-mouse IgG (Invitrogen) antibodies were used at 1:200 and 1:2500 dilutions, respectively. Densitometry of Western blot signals was performed using the gel analysis method of ImageJ (version 1.47) after scanning the photographic films in grayscale at 400 dpi on an Epson Perfection v700 scanner (Schneider,Rasband & Eliceiri 2012). SDHB signals were normalized to those of beta-actin.

RNA sequence database analysis

BAM sequence alignment files of RNA-seq reads mapped against the GRCh37/hg19 human genome assembly were downloaded from public data repositories of the Illumina® BodyMap 2.03 and ENCODE human transcriptome projects (Derrien, et al., 2012,Tilgner, et al., 2012). The two projects have analyzed poly-A+ RNA using the Illumina® HiSeq 2000 or Genome Analyzer II or IIx RNA sequencing platforms. From the BodyMap project, data for all 16 tissues from different healthy individuals was obtained. From the ENCODE project, data for 23 different cell-types/cell-lines (22 with biological duplicates) was obtained.

For each BAM file, the mpileup routine in samtools7 0.1.19 (March 2013 release) was used with its default setting, (Li, et al., 2009) which weighs alignment quality and ignores duplicate reads, to identify RNA-seq reads that align against chromosome 1 regions for the 843 b-long coding region of human *SDHB* mRNA (NCBI RefSeq8 no. NM_003000.2). The output of mpileup was then scanned with a Python 2.7 script to quantify the number of RNA-seq reads with one of five base calls (A, C, G, T or ambiguous) at each nucleotide position. The fraction of RNA-seq reads with a base call of T

for c.136C was compared against the fraction with a base call of T at any of the 213 C nucleotide-bearing positions of the *SDHB* coding region. Statistical significance of any difference was determined with two-tailed Chi-square test with Yates correction using Prism 6.0c software (GraphPad, La Jolla, CA).

None of the 67 single nucleotide polymorphisms (SNPs) that have been documented for the *SDHB* coding region in dbSNP10 database (04-25-2012 release, NCBI dbSNP build 138 phase I) is at the genomic position of *SDHB* c.136C.

Statistical analysis

Unless specified otherwise, statistical analyses of experimental data was performed using the online interface of SISA at http://www.quantitativeskills.com/sisae (Uitenbroek, 2013) using two-tailed non-parametric tests, graphics and descriptive statistics were generated in Excel (version 10; Microsoft, Redmond, WA). Means and standard errors are depicted by horizontal bars in the figures.

RESULTS AND DISCUSSION

Analysis of C136U mutation rate in PBMCs by RT and AS qPCR

To determine the prevalence, distribution, cell type origin and other factors influencing *SDHB* editing, we developed a highly specific and reproducible assay for allele specific quantitative PCR amplification (AS qPCR) of the total and edited C136U *SDHB* mRNAs (see methods). Using this assay, we found that the C136U transcripts were very low or absent in B cell lymphoblastoid and fibroblastic cell lines. The editing occurred at slightly higher levels in PBMCs isolated from fresh blood than in the cell lines (Figure 1A). To study the relative contribution of monocytes and lymphocytes to *SDHB* editing, we performed monocyte enrichment using the well-established cold aggregation method (Mentzer, et al., 1986) with certain modifications (see methods). This method essentially separates PBMCs into cold-aggregating monocyte-enriched and non-aggregating monocyte-depleted (i.e., predominantly lymphocytic) compartments. Monocyte-enriched samples by the cold aggregation method showed higher editing rates than the matched PBMCs (2.16% versus 1.48%, n=36, $P=1.6X10^{-5}$, Wilcoxon matched pairs signed ranks test) and than the matched monocyte-depleted samples (1.47% versus 0.58%, n=10, P=0.005, Wilcoxon matched pairs signed ranks test) (Figure 1A). To further confirm monocyte-origin of the edited transcripts, we isolated peripheral blood monocytes to >92% purity by CD14+ microbeads and tested the mutation rates in three samples. In each sample, a higher mutation rate was found in the monocytes than the CD14- lymphocytes (average 0.84% vs 0.38%). A positive but weak correlation was found between the CD14+ monocyte-fraction and the C136U editing rate in cold-aggregated PBMC samples (Figure 1B). These results indicate that C136U editing occurs in freshly isolated monocytes in low but statistically significantly higher rates than in lymphocytes.

C136U editing rate increases during short-term culture of PBMCs in a time-dependent manner

We cultured monocyte-enriched PBMCs for *in vitro* macrophage differentiation by plate adherence in the presence of 10% fetal bovine serum (FBS) at standard culture conditions as described (Roiniotis, et al., 2009). Flow cytometry showed that the fraction of CD14+ cells among the adherent cells on culture days 5-6 (25.9% ± 5.2%; n=4) was comparable to the uncultured monocyte-enriched PBMC samples (27.2%± 2.7%; n=10). Initial cultures showed that the fraction of the edited transcripts increased in the adherent cells on days 5-7 then decreased to baseline levels on later days (Supplemental Figure S1A). Short-term cultures showed that the editing rates were lower in the first three days than on days 5-7 (3.54% versus 11.62%, n=15, $P=8X10^{-4}$, Wilcoxon matched pairs signed ranks test, Figure 1C). The uncultured monocyte-enriched PBMC samples had lower C136U editing rates than their matched cultures on days 5 and 6 in 17 of the 17 samples (1.7% ± 0.2% versus 10.06% ± 0.8%; $P=2.9X10^{-4}$, Wilcoxon matched pairs signed ranks test). To confirm monocyte origin of the edited transcripts in the cultured samples, we performed flow cytometric sorting of the attached CD14+ cells from culture days 5-8 which essentially separated monocyte/macrophages from lymphocytes to >95% purity. In five of five samples, the CD14+ cells showed higher editing rates than the CD14- cells (Figure 1D). The editing rate was higher among the adherent cells than those in the supernatant (Figure 1E). Collectively, these findings indicate that C136U editing is induced in monocyte/macrophage lineage cells during culture of monocyte-enriched PBMCs in a time-dependent manner.

The maximum mutation rate reached on days 4-8 varied markedly among samples from 1.2% to 18.8%. Total number of cultured cells per well correlated positively but very weakly with the maximum mutation rate (Supplemental Figure S1B). The maximum C136U editing rate trended higher when the total number of monocyte-enriched PBMCs was over 21 million per well versus 20 million or less per well, though this difference did not reach statistical significance (10.9% ± 1.23%; n=16 versus 8.54% ± 1.03%; n=15; P=0.1; Mann Whitney U test, one-tailed).

Morphologic evaluation of cultures associated with C136U editing

We noted the development of three dimensional adherent aggregates (AAs) in monocyte-enriched PBMC cultures, especially in those that had the highest C136U editing rates. These aggregates were detectable within 12 hours and increased in density and size up to a week in culture (Figure 2A and 2B). Hourly photographic imaging in the first two days showed that the aggregates start as a loose collection of cells and become larger and more compact by merging and recruitment of individual cells (Supplemental video S1). Cultures with low AA densities showed lower mutation rates than those with intermediate or high AA densities (n=16, P=0.015, Mann-Whitney U test; Figure 2C).

Morphologic examination showed that the AAs were primarily comprised of intermediate-size cells that generally had round non-convoluted nuclei and a moderate amount of cytoplasm. Occasional lymphocytes and large monocytoid cells with curved nuclei were also noted within the aggregates. In contrast, numerous individually attached macrophages, including those with spindle-like morphology or multi-nucleation, had more abundant cytoplasm compared to cells in the AAs (Figure 2D). Immunostaining with an anti-CD163 antibody confirmed that most cells in the AAs were aggregated monocytes/macrophages (Figure 2E). These results suggest that C136U editing primarily occurs in aggregating monocytes that are in the process of differentiating to macrophages.

Microarray analysis of differentially expressed genes associated with increased C136U editing in normoxia

We performed pairwise microarray gene expression analysis of four sets of low-editing (day 3) and high-editing (day 5-8) samples cultured in normoxia (Table 1) to evaluate (a) global changes in cellular pathways; (b) whether adherent aggregates are associated with micro-environmental hypoxia; and (c) changes in the SDH subunit and cytidine deaminase family of genes. Analysis showed that 171 genes were upregulated and 123 genes were downregulated genes by at least two-fold at a statistically significant level ($P < 0.05$). The subset of these genes (n=55) that showed ≥ fold-change is shown in Supplemental Table S3. The complete list is available on GEO database under accession number GSE45900. No SDH subunit or APOBEC family gene met these criteria. Cytidine deaminase (*CDA*) was the only gene from the cytidine deaminase family of genes that had its expression level changed significantly, with a 3.1-fold increase. qPCR analysis confirmed upregulation of *CDA* expression (average 3.7-fold) and little change in *SDHB* expression (average 0.98-fold) in the high-editing samples relative to the low-editing ones. Significant gene expression changes coordinately occurred in functionally related genes in several Gene Ontology (GO) categories (n=159). This number decreased to 10 after Bonferroni correction for multiple testing was applied (Supplemental Table S4). These 10 categories included defense to wounding, inflammatory, immune and defense responses, taxis, chemotaxis, carboxylic and organic acid transport, locomotory behavior and regulation of cell proliferation. Notably, hypoxia-response genes were not categorically different between the low and the high editing samples. These results indicate that significant gene expression changes occur in inflammatory and immune response pathways during increase in *SDHB* editing and that *CDA* is a candidate gene for enzymatic C136U deamination.

Flow cytometric characterization of cultures associated with C136U editing

To evaluate monocyte macrophage maturation in PBMC culture, we performed flow cytometric characterization of the attached cells using monocyte/macrophage-associated antibodies for CD14, CD16, CD163, HLA-DR and CD206, a mannose receptor associated with M2 type macrophage polarization that promotes wound healing (Porcheray, et al., 2005).

Cold-aggregated uncultured PBMCs showed a discrete and relatively uniform monocytic population that is positive for CD14, HLA-DR and CD163; but negative for CD206 and largely negative for CD16 (Figure 3). Cultured adherent cells at day 6, which showed an increased editing rate, contained a CD14+ population comprised of larger cells with more complexity and were dim-positive for CD206, heterogeneously positive for CD14 and brightly positive for HLA-DR. CD16 and CD163 patterns were similar and showed a heterogeneous negative-to-positive range. Analysis of the adherent cells at day 15, when the editing rates are typically low and the AAs are loose (Supplemental Figure S1C), showed a mature macrophage population that had increased complexity and a more uniform antigenic profile, including homogenous positivity for CD14, CD16, CD163, HLA-DR and CD206. Taken together, these results demonstrate that high C136U editing peaks during monocyte macrophage differentiation in normoxic culture.

C136U editing in cytokine-treated PBMC cells and in monocytic leukemia cell line THP-1

When monocyte-enriched PBMC cultures were treated with M-CSF and GM-CSF/IL4 to facilitate macrophage and dendritic cell differentiation, respectively, lower editing rates were seen compared to the control cultures that contained only 10% FBS ($P=0.012$, $n=8$, and $P=0.04$, $n=5$, respectively, Wilcoxon matched pairs signed ranks test Supplemental Figure S1D). We also tested C136U editing

rates in the monocytic leukemia cell line THP-1. We added macrophage differentiation agents to the media with 10% FBS including phorbol ester PMA, retinoic acid and vitamin D. Significant C136U editing was not identified (less than 1%) either in the untreated THP-1 cell line or after treatment with the differentiating agents. Similarly, hypoxia exposure of the THP-1 cell line showed no increase in C136U levels on days 1, 2 and 3 (less than 1%). These results indicate that C136U editing primarily occurs in mature monocytes during differentiation to macrophages in the presence of serum under normoxic culture conditions and that cytokine-driven macrophage or dendritic cell differentiation or leukemic transformation reduces editing rates.

Induction of C136U editing by hypoxia

Because tissues with inflammation and infarction harboring monocyte/macrophage lineage cells are often hypoxic and because monocyte-macrophage differentiation occurs in tissues where oxygen pressure is lower than that in blood (Roiniotis, et al., 2009), we evaluated the role of hypoxia on C136U editing. We observed that monocyte-enriched PBMC cultures in hypoxia did not develop the firmly adherent aggregates associated with high editing rates in the normoxic cultures and that essentially all cells were in suspension. The fraction of viable CD14+ monocytes in the hypoxic supernatants on culture day 2 was similar to the original uncultured samples as evaluated by flow cytometry (20.9% versus 20.4%, n=4). The editing rate in the hypoxic cultures increased in the first three days with a peak on day 2, when it is typically low in the normoxic control cultures (Figure 1C and 4A). In five of the 14 samples, C136U editing rates were higher (21%-49%) than in any normoxic culture. Hypoxia increased the fraction of C136U transcripts by 0.4% to 46% on culture day 2. Pairwise comparison of the editing rates in supernatant cells in hypoxia versus total cells in normoxia from 14 different samples in the first three days showed marked upregulation of C136U editing by hypoxia ($P=2X10^{-7}$, n=42, Wilcoxon matched pairs test; Fig. 4B). Hypoxia increased

C136U fractions in 39 of 42 pairwise comparisons from 14 samples cultured in normoxia and hypoxia for three days. Comparison of the flow sorted CD14+ and CD14– cell populations confirmed that monocytes were the main source of C136U editing in hypoxia (Figure 4E). RT-qPCR analysis showed marked upregulation of *CDA* (average 7.5-fold change on day 2, n=6) and downregulation of *SDHB* (average 0.37-fold change on day 3, n=6) in the hypoxic cultures relative to the control gene beta 2 microglobulin. Western blot analysis of a monocyte-enriched PBMC sample cultured in normoxic and hypoxic conditions showed no marked changes in the expression SDHB protein product (Figure 4D), suggesting that the impact of C136U editing on protein expression levels is subtle and quantitative. The variable increase in the percentage of C136U transcripts by hypoxia could be caused by unknown technical or biological factors including variable fraction of monocytes in donors, variation in inherent enzymatic activity of the putative editing enzyme or nonsense mediated decay pathway activation.(Chang, Imam & Wilkinson 2007).

Analysis of genomic DNA for C136T editing

To test whether the C136U RNA mutation has a corresponding C-to-T genomic DNA mutation in *SDHB* exon 2, we compared mutant RNA and DNA levels using our previously described semi-quantitative method based on PCR amplification and *Taq*1 restriction enzyme digestion (Baysal 2007). We found no evidence of a corresponding DNA mutation in the hypoxic samples containing high levels of C136U RNA mutations (Figure 4C). These results indicate that C136U mRNA editing occurs during or after transcription.

High throughput sequencing of *SDHB* and *SDHD* transcripts

To obtain a global view of transcript editing in the *SDHB* and the *SDHD* genes, we performed high throughput sequencing of the full length coding transcripts obtained by RT and high-fidelity PCR.

We sequenced the four pairs of normoxic cultures that were characterized by microarray gene expression analyses. Each pair derived from the same PBMC and contained a sample with a low C136U editing rate (day 3 culture) and a sample with a high C136U editing rate (day 5-8 culture). Interrogation of the transcript sequences confirmed C136U mutations in each of the high-editing-rate sample. On average, 40% higher editing levels were seen by high throughput sequencing than those estimated by AS qPCR (Table 1). No additional canonical RNA edits in the form of A-to-I/G or C-to-U/T changes were identified in the *SDHB* transcripts. No additional *SDHB* transcript variants could be identified by Sanger sequencing. In contrast, Sanger sequencing confirmed C136U in all four samples that showed high editing rates by AS qPCR and by high-throughput sequencing (Supplemental Figure S1E). Similarly, *SDHD* transcripts showed no evidence of RNA editing by high-throughput sequencing. Taken together, these results demonstrate that *SDHB* C136U editing is not accompanied by other transcript variants either in *SDHB* or *SDHD* and suggest that a site-specific C-to-U RNA editing mechanism regulates the *SDHB* functional transcript dosage.

Analysis of transcriptome sequence databases

We examined RNA sequencing data of the Illumina Human Body Map and ENCODE Human Transcriptome projects (Derrien, et al., 2012; Tilgner, et al., 2012; Brazma, et al., 2003) for sequence variations in the ORF region *SDHB* mRNA. As expected, among the 16 normal human tissues from Human Body Map, the highest levels of *SDHB* C136U editing was seen in white blood cells (1.7%), with the other 15 tissues showing an average editing level of 0.2% (SD=0.3%), with ovary (1%) and kidney (0.9%) being those with the highest levels among the 15 (Supplemental Table S5). Among the 45 samples of 23 different cell-types of the ENCODE set, the editing rate was highest for the two primary CD14+ monocytes (1.9% and 2.6%), with the other samples showing an average 0.1% (SD=0.2%) editing rate (Supplemental Table S6). The editing rates noted for the samples for white

blood cells and the monocytes are unlikely to be a result of sequencing error since a base call of U instead of C was made in only 0.04%-0.09% of the reads when all 213 C-bearing positions of the *SDHB* coding region were examined ($P < 0.001$, Chi square test). These results support our earlier conclusions that C136U editing occurs at low but statistically significant levels in peripheral blood monocytes.

CONCLUSIONS

We found that an acquired RNA nonsense mutation (R46X) introduced by C-to-U RNA editing dynamically reduces the *SDHB* functional transcript dosage in monocytes during early macrophage differentiation and upon short-term exposure to hypoxia. The fraction of C136U transcripts was variable in monocyte-enriched PBMC cultures and peaked around 19% in normoxic cultures but increased to up to 49% within 2 days in hypoxia. The editing rates must be higher in pure monocytes because CD14+ cell isolation increased the percentages of C136U transcripts by 1.25-fold in normoxic cultures and 1.68-fold in hypoxic cultures. Gene expression analyses identified *CDA* as a candidate gene for *SDHB* editing. To our knowledge, these results provide the first examples of hypoxia-inducible coding RNA editing and a programmed mutation targeting an endogenous nuclear gene in myeloid cells.

On the basis of genetic studies on SDH-mutated paragangliomas that show constitutive activation of hypoxia-inducible pathways, we hypothesize that reduction in the *SDHB* dosage by RNA editing facilitates hypoxia adaptation in monocytes by amplifying hypoxia signaling from mitochondria. We speculate that the programmed *SDHB* RNA editing during normoxic macrophage differentiation might serve to augment signaling of inflammatory hypoxia. Although the precise mechanisms linking hypoxia sensing and signaling to *SDHB* RNA editing remain to be determined, parallels can

be drawn between the monocytes circulating in the high-oxygen environment of the peripheral blood and subsequently migrating into the hypoxic areas where differentiation into macrophages occurs versus certain facultatively aerobic organisms such as the intestinal parasitic worm *Ascaris suum* (*A. suum*). *A. suum* spores living in open air are exposed to high oxygen concentrations and utilize SDH; whereas parasitic adult worms living in the hypoxic environment of intestine use fumarate reductase (Kita, et al., 2002). Thus, suppression of SDH might be an evolutionarily conserved metabolic adaptation to hypoxia achieved by diverse molecular mechanisms and might contribute to increased monocyte/macrophage survival observed under hypoxia due to enhanced glycolysis (Roiniotis, et al., 2009).

More broadly, our results extend previous observations associating external factors with differential A-to-I RNA editing (Garrett & Rosenthal 2012; Balik, et al., 2013; Sanjana, et al., 2012) and demonstrate in a robust experimental model that C-to-U coding RNA editing of certain genes occurs dynamically in a cell type and environment-dependent manner. Our findings suggest that gene targets of RNA editing could be missed by whole transcriptome sequence analyses unless tissues are examined in their physiologically relevant different states. If the threshold for significant RNA editing is set at 10% or more in whole transcriptome sequence analyses (for example in Park, et al., 2012), the *SDHB* gene would be identified as a target of RNA editing in monocytes only upon exposure to hypoxia or during macrophage differentiation but not in peripheral blood.

If *SDHB* editing aberrantly occurs in the paraganglionic tissues, an increased risk of paraganglioma development might ensue. Recent evidence suggests that tumor suppressor gene functions can be compromised by as little as a 20% decrease in gene dosage (Berger, Knudson & Pandolfi 2011). Dosage sensitivity of the SDH complex is specifically supported by the imprinted transmission of PGL tumors by *SDHD* mutations as paternal but not maternal transmission of *SDHD* mutations is

known to cause highly penetrant tumors. Recent discovery of tissue-specific imprint marks in the vicinity of *SDHD* suggests that subtle allelic expression differences can result in discordant penetrances depending on which allele carries the mutation (Baysal, et al., 2011). If programmed downregulation of *SDHB* by RNA editing improves monocyte survival in hypoxic environments, therapeutic manipulation of this pathway might provide a tool to modify risk in common diseases associated with macrophage infiltration.

FIGURE LEGENDS

Figure 1 *SDHB* C136U RNA editing is induced in monocytes during short-term culture. **(A)** C136U editing is measured in 9 lymphoblastoid cell lines and one fibroblastic cell line, freshly isolated PBMCs (n=50), PBMCs monocyte-enriched by cold-aggregation (Mono+; n=42) and monocyte-depleted PBMCs comprised of largely lymphocytes (Mono-; n=10). Horizontal lines represent mean ± standard errors throughout the figures. **(B)** Fraction of the C136U transcripts weakly correlates with the CD14+ monocyte percentage in monocyte-enriched PBMCs (Pearson correlation coefficient r=0.36). **(C)** Impact of short-term culture on C136U editing. Short-term culture of five monocyte-enriched PBMCs shows upregulation of C136U editing in adherent cells in culture days 5-7 compared to days 1-3. Day 0 represents the uncultured samples. **(D)** Flow cytometric sorting of CD14+ versus CD14- adherent cells on culture days 5-8 shows higher mutation rates in monocyte-macrophage lineage than in lymphocytes (P=0.04, n=5, Wilcoxon matched pairs signed ranks test). **(E)** C136U editing is lower among non-adherent cells in the supernatant than in adherent cells (4.3% versus 9.8%) on culture days 5-7 (n=19 wells from 11 samples on days 5-7, $P=2.1 \times 10^{-4}$, Wilcoxon matched pairs signed ranks test).

Figure 2 *SDHB* C136U RNA editing rate correlates with adherent monocyte-rich adherent aggregates (AA) in normoxic culture. The AAs on culture days 1 **(A)** and 5 **(B)** are shown (5X low power field; vertical bars equal to 1 mm). The culture is initiated with 30 million cells per well. The AAs grow in size until approximately days 5-7 when the C136U editing rate also usually peaks. **(C)** High editing rates are seen in cultures with intermediate and high density of adherent aggregates. Aggregate densities are grouped as follows: Low= less than 10 aggregates/per 5X low power field (lpf); Intermediate=10-20 aggregates/lpf; High= more than 20 aggregates/lpf **(D)** Giemsa stain

highlights an adherent aggregate on day 6 culture. Individually attached mature macrophages have mostly round eccentric nuclei and abundant cytoplasm. Occasional multi-nucleated macrophages (arrowheads) and rare small lymphocytes (green arrows) are also present. Macrophages within the aggregate are smaller with less cytoplasm and occasionally have curved nuclei (arrows). **(E)** CD163 immunostaining of adherent aggregates. Immunocytochemical staining for monocyte-macrophage-specific antigen CD163, a scavenger receptor for hemoglobin-haptoglobin complex, demonstrates that the adherent aggregates are primarily comprised of monocyte/macrophage lineage cells. Individually attached macrophages outside the aggregate also stain with variable intensity (short arrows); while numerous small lymphocytes are negative (long arrows).

Figure 3 *SDHB* C136U RNA editing increases during monocyte-macrophage maturation. Flow cytometric evaluation of monocyte-macrophage maturation is shown in uncultured cold aggregated PBMCs (first column), adherent cells on culture day 6 (second column) and adherent cells on culture day 15 (third column). The day 15 culture shows a relatively homogenous large (indicated by high forward scatter, FSC-A) macrophage population that has high complexity (indicated by high side scatter, SSC-A) and is positive for CD206 (mannose receptor), HLA-DR and CD163. In contrast, uncultured monocytes are largely a uniform population that is smaller with less complexity and is negative for CD206. The day 6 culture, which has 11.6% C136U editing rate, shows a CD14+ population that is brightly positive for HLA-DR, dim-positive for CD206 and negative for CD163. CD14+ monocyte-macrophage and lymphocyte populations are marked by green and red, respectively.

Figure 4 Hypoxia induces *SDHB* C136U RNA editing. **(A)** The editing rates are higher on days 1-3 in hypoxia and on days 5, 6 in normoxia. The average of four independent cultures is presented. **(B)** C136U editing rates in 12 independent cultures in hypoxia versus normoxia during 3 days of culture are shown. The editing rates were obtained from supernatant in all hypoxic cultures (first column) and from total cell population in normoxic cultures, except in two normoxic cultures where only supernatant was collected (second column). D0 samples represent the original uncultured cold aggregated PBMCs. **(C)** PCR amplification and *Taq*1 restriction enzyme (RE) digestion shows no evidence of C136T DNA mutation in *SDHB* exon 2 genomic DNA (gDNA) (right panel) in the same samples with high C136U RNA editing rates (left panel). The C13U RNA editing rates above the lanes were measured by AS qPCR. RT- and gDNA-PCRs generate amplicon sizes of 285 bp and 233 bp, respectively. *Taq*1 RE digestion of wild type cDNA and gDNA sequences generates 159 bp/126 bp and 131 bp/102 bp bands, respectively. C136U/T mutation destroys the RE site. **(D)** Western blot analysis of normoxic (N) and hypoxic (H) cultures from one donor shows no major changes in SDHB protein expression, normalized against beta actin, as the editing rate increases in hypoxia, but possibly a subtle decrease when the C136U percentage is 16.1% on day 2 in hypoxia. Hypoxic cultures were sampled twice a day, 10 h apart. **(E)** The editing rates are shown for flow sorted CD14+ and CD14- viable cells from day 2 hypoxic cultures (n=4). In all experiments, hypoxic and control normoxic culture derive from the same donor (i.e., oxygen tension is the only variable).

AUTHORSHIP

BEB conceptualized the study and wrote the manuscript. BEB, RT, JW and PKW designed experiments. RT, KDJ and BEB performed experiments. BL and JW performed the bioinformatic analysis of microarray expression data. SP performed the ENCODE and Illumina database analysis. All authors approved the final manuscript.

ACKNOWLEDGMENTS

We thank anonymous platelet donors, personnel at RPCI's core facilities for assistance with flow cytometry, high-throughput sequencing, immunocytochemistry and hypoxia treatment, Eric Kannisto for technical help, and the Department of Pathology and Laboratory Medicine for administrative and financial support.

CONFLICT OF INTEREST DISCLOSURE

The authors declare no conflict of interest.

Supplemental material

Supplemental Figure legends

Supplemental Figure S1 (A) Impact of long-term culture and cell density on C136U editing are shown. Five monocyte-enriched PBMCs were cultured long-term and the C136U editing rates were measured. The editing rate was higher in adherent cells on days 5-7 than in the uncultured monocyte-enriched PBMCs and on days 12-14 and 19-21 (P=0.017, n=5, one-way ANOVA). **(B)** Maximum C136U editing rate in the adherent cells shows very weakly positive correlation with the total number of monocyte-enriched PBMCs per well. Total number of samples=31. **(C)** Attached aggregates (AAs) on culture day 20 are shown. The AAs start loosening after one week in culture and eventually appear as flat areas of increased cellular density. This culture was fed with fresh RPMI-1640/10% FBS on day 8.

(D) Cytokine mediated differentiation towards macrophages or dendritic cells reduce C136U editing rates. Cultures containing 10% FCS showed higher mutation rates than those treated with M-CSF (p=0.012) or GM-CSF/IL4 (p=0.04). Multi-day averages from two PBMC cultures are shown. Matched samples were collected on days 4-8 for the m-CSF culture (n=8) and days 4-6 for the GM-CSF/IL4 cultures (n=5). The editing rate was obtained from adherent cells in 10% FCS and m-CSF treated (macrophage-differentiation) wells and from non-adherent cells in supernatant in GM-CSF/IL4-treated (dendritic cell-differentiation) wells.

(E) Sanger sequencing confirms C136U RNA editing in all four samples that showed high editing rates by RT-qPCR and high-throughput sequencing. Chromatograms show examples of a sample with a low editing rate (sample 1, day3 in Table 1) and one with a high editing rate (sample 4, day 7 in Table 1). C136U variant is shown by arrows.

Supplemental Video S1 Culture is initiated after mild monocyte enrichment by cold aggregation. After 5 hours the supernatant is removed and hourly photographic imaging is started. Video is a composite of sequential images (time-lapse) for the first 48 hours. Note that the aggregates start as a loose collection of cells and become larger and more compact by cell recruitment.

References

Astrom K, Cohen JE, Willett-Brozick JE, Aston CE, Baysal BE. 2003. Altitude is a phenotypic modifier in hereditary paraganglioma type 1: evidence for an oxygen-sensing defect. *Human Genetics* **113**: 228.

Balik A, Penn AC, Nemoda Z, Greger IH. 2013. Activity-regulated RNA editing in select neuronal subfields in hippocampus. *Nucleic Acids Research* **41**: 1124.

Bayley JP, Devilee P, Taschner PE. 2005. The SDH mutation database: an online resource for succinate dehydrogenase sequence variants involved in pheochromocytoma, paraganglioma and mitochondrial complex II deficiency. *BMC Medical Genetics* **6**: 39.

Baysal BE. 2007. A recurrent stop-codon mutation in succinate dehydrogenase subunit B gene in normal peripheral blood and childhood T-cell acute leukemia. *PloS One* **2**: e436.

Baysal BE, Ferrell RE, Willett-Brozick JE, Lawrence EC, Myssiorek D, Bosch A, van der Mey A, Taschner PE, Rubinstein WS, Myers EN, Richard CW,3rd, Cornelisse CJ, Devilee P, Devlin B. 2000. Mutations in SDHD, a mitochondrial complex II gene, in hereditary paraganglioma. *Science (New York, N.Y.)* **287**: 848.

Baysal BE, McKay SE, Kim YJ, Zhang Z, Alila L, Willett-Brozick JE, Pacak K, Kim TH, Shadel GS. 2011. Genomic imprinting at a boundary element flanking the SDHD locus. *Human Molecular Genetics* **20**: 4452.

Berger AH, Knudson AG, Pandolfi PP. 2011. A continuum model for tumour suppression. *Nature* **476**: 163.

Blanc V, Davidson NO. 2003. C-to-U RNA editing: mechanisms leading to genetic diversity. *The Journal of Biological Chemistry* **278**: 1395.

Brazma A, Parkinson H, Sarkans U, Shojatalab M, Vilo J, Abeygunawardena N, Holloway E, Kapushesky M, Kemmeren P, Lara GG, Oezcimen A, Rocca-Serra P, Sansone SA. 2003. ArrayExpress--a public repository for microarray gene expression data at the EBI. *Nucleic Acids Research* **31**: 68.

Burnichon N, Abermil N, Buffet A, Favier J, Gimenez-Roqueplo AP. 2012. The genetics of paragangliomas. *European Annals of Otorhinolaryngology, Head and Neck Diseases* **129**: 315.

Cerecer-Gil NY, Figuera LE, Llamas FJ, Lara M, Escamilla JG, Ramos R, Estrada G, Hussain AK, Gaal J, Korpershoek E, de Krijger RR, Dinjens WN, Devilee P, Bayley JP. 2010. Mutation of SDHB is a cause of hypoxia-related high-altitude paraganglioma. *Clinical Cancer Research : an official journal of the American Association for Cancer Research* **16**: 4148.

Chang YF, Imam JS, Wilkinson MF. 2007. The nonsense-mediated decay RNA surveillance pathway. *Annual Review of Biochemistry* **76**: 51.

Dahia PL, Ross KN, Wright ME, Hayashida CY, Santagata S, Barontini M, Kung AL, Sanso G, Powers JF, Tischler AS, Hodin R, Heitritter S, Moore F, Dluhy R, Sosa JA, Ocal IT, Benn DE, Marsh DJ, Robinson BG, Schneider K, Garber J, Arum SM, Korbonits M, Grossman A, Pigny P, Toledo SP, Nose V, Li C, Stiles CD. 2005. A HIF1alpha regulatory loop links hypoxia and mitochondrial signals in pheochromocytomas. *PLoS Genetics* **1**: 72.

Derrien T, Johnson R, Bussotti G, Tanzer A, Djebali S, Tilgner H, Guernec G, Martin D, Merkel A, Knowles DG, Lagarde J, Veeravalli L, Ruan X, Ruan Y, Lassmann T, Carninci P, Brown JB, Lipovich L, Gonzalez JM, Thomas M, Davis CA, Shiekhattar R, Gingeras TR, Hubbard TJ, Notredame C, Harrow J, Guigo R. 2012. The GENCODE v7 catalog of human

626 long noncoding RNAs: analysis of their gene structure, evolution, and expression. *Genome*
627 *Research* **22**: 1775.

628 **Du P, Kibbe WA, Lin SM. 2008.** lumi: a pipeline for processing Illumina microarray.
629 *Bioinformatics (Oxford, England)* **24**: 1547.

630 **Garrett S, Rosenthal JJ. 2012.** RNA editing underlies temperature adaptation in K+ channels
631 from polar octopuses. *Science (New York, N.Y.)* **335**: 848.

632 **Guzy RD, Sharma B, Bell E, Chandel NS, Schumacker PT. 2008.** Loss of the SdhB, but Not
633 the SdhA, subunit of complex II triggers reactive oxygen species-dependent hypoxia-inducible
634 factor activation and tumorigenesis. *Molecular and Cellular Biology* **28**: 718.

635 **Huang da W, Sherman BT, Lempicki RA. 2009.** Systematic and integrative analysis of large
636 gene lists using DAVID bioinformatics resources. *Nature Protocols* **4**: 44.

637 **Kaelin WG,Jr, Ratcliffe PJ. 2008.** Oxygen sensing by metazoans: the central role of the HIF
638 hydroxylase pathway. *Molecular Cell* **30**: 393.

639 **Kita K, Hirawake H, Miyadera H, Amino H, Takeo S. 2002.** Role of complex II in anaerobic
640 respiration of the parasite mitochondria from Ascaris suum and Plasmodium falciparum.
641 *Biochimica et Biophysica Acta* **1553**: 123.

642 **Kleinman CL, Adoue V, Majewski J. 2012.** RNA editing of protein sequences: a rare event in
643 human transcriptomes. *RNA (New York, N.Y.)* **18**: 1586.

644 **Li H, Handsaker B, Wysoker A, Fennell T, Ruan J, Homer N, Marth G, Abecasis G, Durbin**
645 **R, 1000 Genome Project Data Processing Subgroup. 2009.** The Sequence Alignment/Map
646 format and SAMtools. *Bioinformatics (Oxford, England)* **25**: 2078.

647 **Livak KJ, Schmittgen TD. 2001.** Analysis of relative gene expression data using real-time
648 quantitative PCR and the 2(-Delta Delta C(T)) Method. *Methods (San Diego, Calif.)* **25**: 402.

649 **Mentzer SJ, Guyre PM, Burakoff SJ, Faller DV. 1986.** Spontaneous aggregation as a
650 mechanism for human monocyte purification. *Cellular Immunology* **101**: 312.
651 **Muller M, Mentel M, van Hellemond JJ, Henze K, Woehle C, Gould SB, Yu RY, van der**
652 **Giezen M, Tielens AG, Martin WF. 2012.** Biochemistry and evolution of anaerobic energy
653 metabolism in eukaryotes. *Microbiology and Molecular biology Reviews : MMBR* **76**: 444.
654 **Nishikura K. 2010.** Functions and regulation of RNA editing by ADAR deaminases. *Annual*
655 *Review of Biochemistry* **79**: 321.
656 **Park E, Williams B, Wold BJ, Mortazavi A. 2012.** RNA editing in the human ENCODE
657 RNA-seq data. *Genome Research* **22**: 1626.
658 **Piskol R, Peng Z, Wang J, Li JB. 2013.** Lack of evidence for existence of noncanonical RNA
659 editing. *Nature Biotechnology* **31**: 19.
660 **Porcheray F, Viaud S, Rimaniol AC, Leone C, Samah B, Dereuddre-Bosquet N, Dormont**
661 **D, Gras G. 2005.** Macrophage activation switching: an asset for the resolution of inflammation.
662 *Clinical and Experimental Immunology* **142**: 481.
663 **Roiniotis J, Dinh H, Masendycz P, Turner A, Elsegood CL, Scholz GM, Hamilton JA. 2009.**
664 Hypoxia prolongs monocyte/macrophage survival and enhanced glycolysis is associated with
665 their maturation under aerobic conditions. *Journal of Immunology (Baltimore, Md.: 1950)* **182**:
666 7974.
667 **Rutter J, Winge DR, Schiffman JD. 2010.** Succinate dehydrogenase - Assembly, regulation and
668 role in human disease. *Mitochondrion* **10**: 393.
669 **Saldana MJ, Salem LE, Travezan R. 1973.** High altitude hypoxia and chemodectomas. *Human*
670 *Pathology* **4**: 251.

Sanjana NE, Levanon EY, Hueske EA, Ambrose JM, Li JB. 2012. Activity-dependent A-to-I RNA editing in rat cortical neurons. *Genetics* **192**: 281.

Schneider CA, Rasband WS, Eliceiri KW. 2012. NIH Image to ImageJ: 25 years of image analysis. *Nature Methods* **9**: 671.

Selak MA, Armour SM, MacKenzie ED, Boulahbel H, Watson DG, Mansfield KD, Pan Y, Simon MC, Thompson CB, Gottlieb E. 2005. Succinate links TCA cycle dysfunction to oncogenesis by inhibiting HIF-alpha prolyl hydroxylase. *Cancer Cell* **7**: 77.

Skuse GR, Cappione AJ, Sowden M, Metheny LJ, Smith HC. 1996. The neurofibromatosis type I messenger RNA undergoes base-modification RNA editing. *Nucleic Acids Research* **24**: 478.

Smyth GK. 2004. Linear models and empirical bayes methods for assessing differential expression in microarray experiments. *Statistical Applications in Genetics and Molecular Biology* **3**: Article3.

Tilgner H, Knowles DG, Johnson R, Davis CA, Chakrabortty S, Djebali S, Curado J, Snyder M, Gingeras TR, Guigo R. 2012. Deep sequencing of subcellular RNA fractions shows splicing to be predominantly co-transcriptional in the human genome but inefficient for lncRNAs. *Genome Research* **22**: 1616.

Uitenbroek DG *SISA Binomial*. 2013. http://www.quantitativeskills.com/sisa/distributions/binomial.htm. Last accessed 4/4/2013.

Table 1(on next page)

Percentage of C136U transcripts estimated by allele specific (AS) qPCR and high-throughput amplicon sequencing in normoxic cultures

Table 1

Percentage of C136U transcripts estimated by allele specific (AS) qPCR and high-throughput amplicon sequencing in normoxic cultures

Sample No.	Day in culture	AS qPCR	high-throughput sequencing[a]
1	Day 3	2.2%	NR[b]
1	Day 6	15.9%	22%
2	Day 3	1.3%	NR
2	Day 8	12.3%	23%
3	Day 3	4%	NR
3	Day 6	13.5%	15%
4	Day 3	8.7%	11%
4	Day 7	18.8%	26%

[a] Sequencing depth ranges between 4980 and 4986 for the reported variants.

[b] NR= Not reported. Variants detected by high-throughput sequencing are reported only when their frequency exceeds 10%.

Figure 1

SDHB C136U RNA editing is induced in monocytes during short-term culture.

(A) C136U editing is measured in 9 lymphoblastoid cell lines and one fibroblastic cell line, freshly isolated PBMCs (n=50), PBMCs monocyte-enriched by cold-aggregation (Mono+; n=42) and monocyte-depleted PBMCs comprised of largely lymphocytes (Mono-; n=10). Horizontal lines represent mean ± standard errors throughout the figures. **(B)** Fraction of the C136U transcripts weakly correlates with the CD14+ monocyte percentage in monocyte-enriched PBMCs (Pearson correlation coefficient r=0.36). **(C)** Impact of short-term culture on C136U editing. Short-term culture of five monocyte-enriched PBMCs shows upregulation of C136U editing in adherent cells in culture days 5-7 compared to days 1-3. Day 0 represents the uncultured samples. **(D)** Flow cytometric sorting of CD14+ versus CD14- adherent cells on culture days 5-8 shows higher mutation rates in monocyte-macrophage lineage than in lymphocytes (P=0.04, n=5, Wilcoxon matched pairs signed ranks test). **(E)** C136U editing is lower among non-adherent cells in the supernatant than in adherent cells (4.3% versus 9.8%) on culture days 5-7 (n=19 wells from 11 samples on days 5-7, P=2.1 X10 $^{-4}$, Wilcoxon matched pairs signed ranks test).

Figure 1

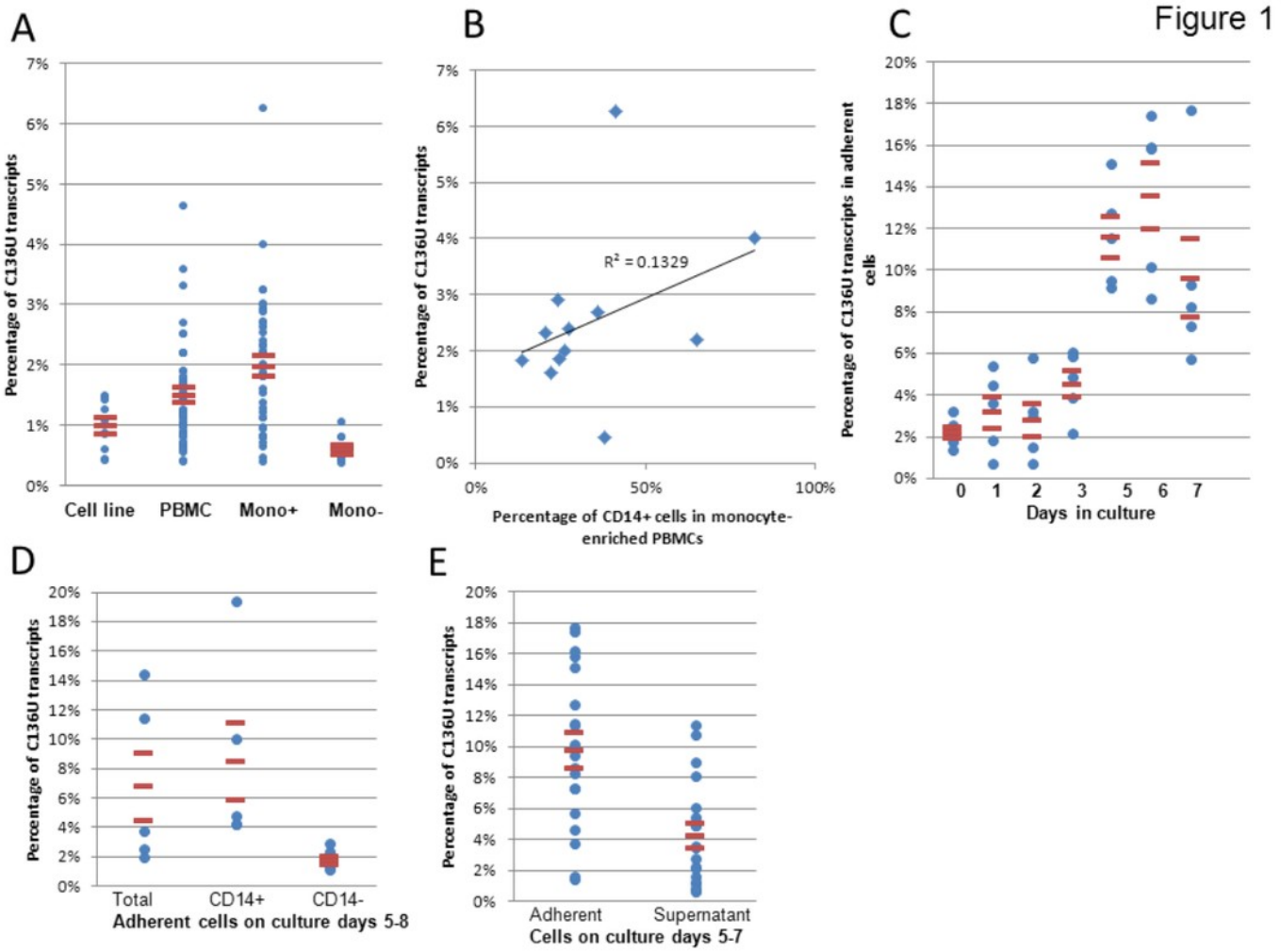

Figure 2

SDHB C136U RNA editing rate correlates with adherent monocyte-rich adherent aggregates (AA) in normoxic culture.

The AAs on culture days 1 **(A)** and 5 **(B)** are shown (5X low power field; vertical bars equal to 1 mm). The culture is initiated with 30 million cells per well. The AAs grow in size until approximately days 5-7 when the C136U editing rate also usually peaks. **(C)** High editing rates are seen in cultures with intermediate and high density of adherent aggregates. Aggregate densities are grouped as follows: Low= less than 10 aggregates/per 5X low power field (lpf); Intermediate=10-20 aggregates/lpf; High= more than 20 aggregates/lpf **(D)** Giemsa stain highlights an adherent aggregate on day 6 culture. Individually attached mature macrophages have mostly round eccentric nuclei and abundant cytoplasm. Occasional multi-nucleated macrophages (arrowheads) and rare small lymphocytes (green arrows) are also present. Macrophages within the aggregate are smaller with less cytoplasm and occasionally have curved nuclei (arrows). **(E)** CD163 immunostaining of adherent aggregates. Immunocytochemical staining for monocyte-macrophage-specific antigen CD163, a scavenger receptor for hemoglobin-haptoglobin complex, demonstrates that the adherent aggregates are primarily comprised of monocyte/macrophage lineage cells. Individually attached macrophages outside the aggregate also stain with variable intensity (short arrows); while numerous small lymphocytes are negative (long arrows).

Figure 2

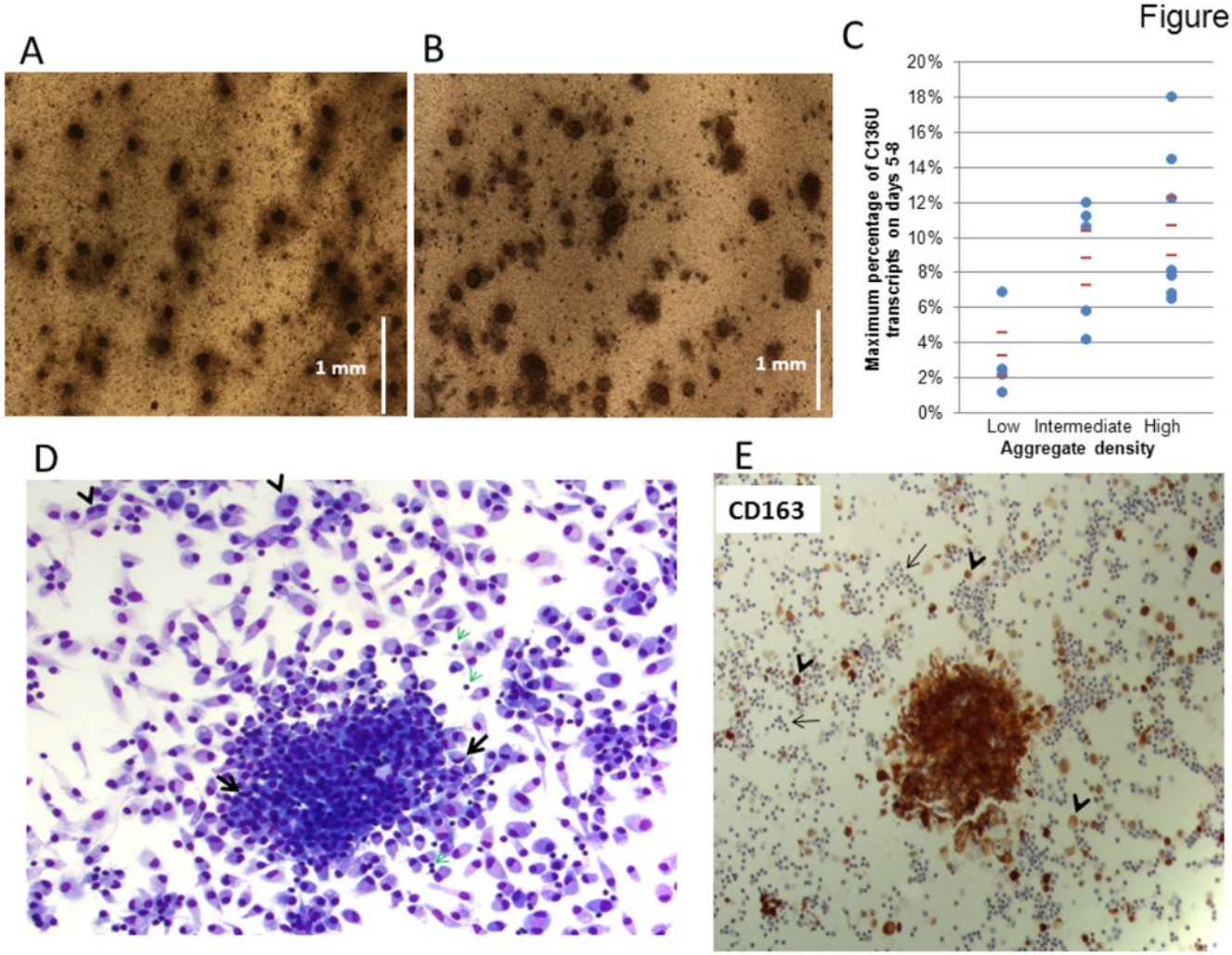

Figure 3

SDHB C136U RNA editing increases during monocyte-macrophage maturation.

Flow cytometric evaluation of monocyte-macrophage maturation is shown in uncultured cold aggregated PBMCs (first column), adherent cells on culture day 6 (second column) and adherent cells on culture day 15 (third column). The day 15 culture shows a relatively homogenous large (indicated by high forward scatter, FSC-A) macrophage population that has high complexity (indicated by high side scatter, SSC-A) and is positive for CD206 (mannose receptor), HLA-DR and CD163. In contrast, uncultured monocytes are largely a uniform population that is smaller with less complexity and is negative for CD206. The day 6 culture, which has 11.6% C136U editing rate, shows a CD14+ population that is brightly positive for HLA-DR, dim-positive for CD206 and negative for CD163. CD14+ monocyte-macrophage and lymphocyte populations are marked by green and red, respectively.

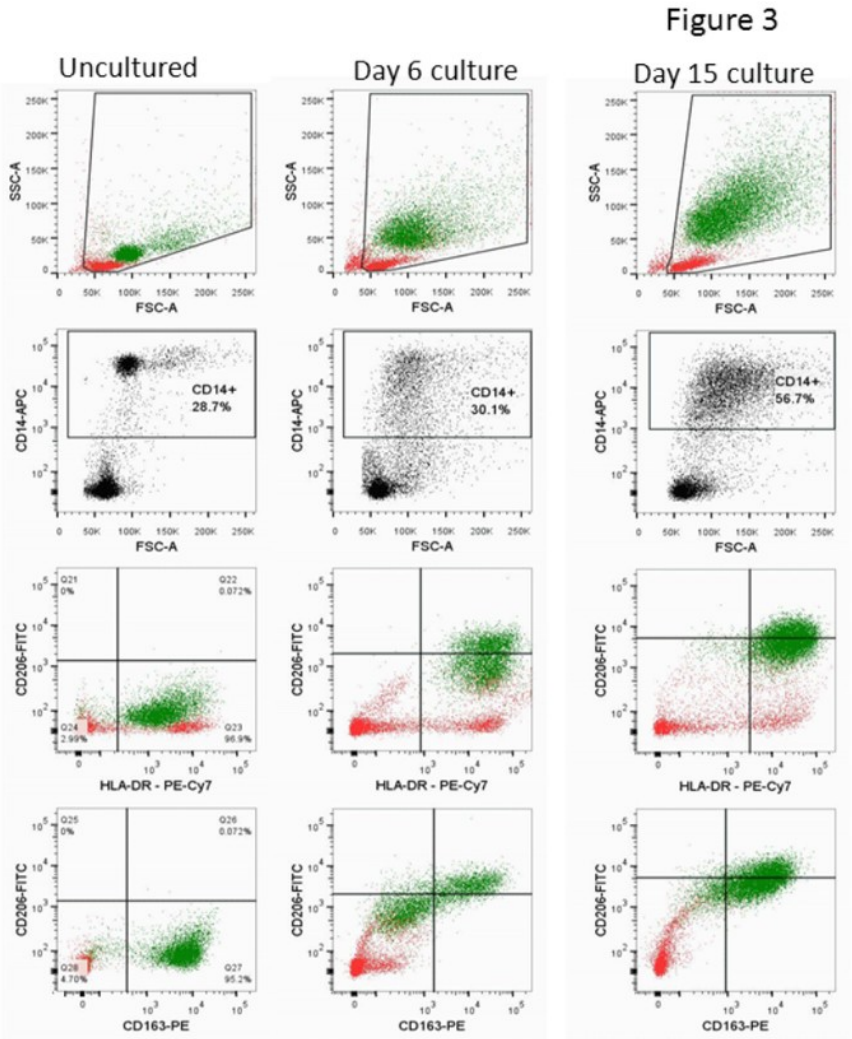

Figure 4

Hypoxia induces *SDHB* C136U RNA editing.

(A) The editing rates are higher on days 1-3 in hypoxia and on days 5, 6 in normoxia. The average of four independent cultures is presented. **(B)** C136U editing rates in 12 independent cultures in hypoxia versus normoxia during 3 days of culture are shown. The editing rates were obtained from supernatant in all hypoxic cultures (first column) and from total cell population in normoxic cultures, except in two normoxic cultures where only supernatant was collected (second column). D0 samples represent the original uncultured cold aggregated PBMCs. **(C)** PCR amplification and *Taq*1 restriction enzyme (RE) digestion shows no evidence of C136T DNA mutation in *SDHB* exon 2 genomic DNA (gDNA) (right panel) in the same samples with high C136U RNA editing rates (left panel). The C13U RNA editing rates above the lanes were measured by AS qPCR. RT- and gDNA-PCRs generate amplicon sizes of 285 bp and 233 bp, respectively. *Taq*1 RE digestion of wild type cDNA and gDNA sequences generates 159 bp/126 bp and 131 bp/102 bp bands, respectively. C136U/T mutation destroys the RE site. **(D)** Western blot analysis of normoxic (N) and hypoxic (H) cultures from one donor shows no major changes in SDHB protein expression, normalized against beta actin, as the editing rate increases in hypoxia, but possibly a subtle decrease when the C136U percentage is 16.1% on day 2 in hypoxia. Hypoxic cultures were sampled twice a day, 10 h apart. **(E)** The editing rates are shown for flow sorted CD14+ and CD14- viable cells from day 2 hypoxic cultures (n=4). In all experiments, hypoxic and control normoxic culture derive from the same donor (i.e., oxygen tension is the only variable).